Calculation of optical properties and density of states for systems with huge unit cells

H.-Ch. Weissker, J. Furthmüller, and F. Bechstedt
Institut für Festkörpertheorie und Theoretische Optik, Friedrich-Schiller-Universität, D-07743 Jena, Germany
(Received 3 January 2001; published 27 June 2001)

We present a method for the *ab initio* calculation of spectral properties of systems with huge unit cells. Translationally invariant systems with elementary cells containing several hundred atoms in the unit cell are characterized by a large number of bands in a very small Brillouin zone. This makes the allocation of energies at different **k** points to one band impossible. For that reason a quadratic extrapolation of the band energies is performed starting from a single **k** point $\mathbf{k}_0$. The band energies and momentum operator matrix elements are calculated at $\mathbf{k}_0$ using the projector augmented wave method. The Brillouin-zone integration is carried out by means of the linear tetrahedron method following a resampling procedure. The viability of the method is demonstrated for nonprimitive large supercells by reproducing the absorption coefficient and the density of states of an ideal crystal. The method is applied to 216- and 512-atom simple-cubic supercells. A germanium cluster embedded in a host material is treated as an example of a perturbed system.

DOI: 10.1103/PhysRevB.64.035105 PACS number(s): 71.20.−b, 73.22.−f, 78.20.Bh

I. INTRODUCTION

Spectral properties of solids are related to the single- or two-particle density of states (DOS). Examples are the optical absorption, the electronic contribution to the heat capacity, and two-phonon Raman spectra. In the crystalline case the corresponding sums over electronic states involve integrations over the Brillouin zone (BZ) which are commonly carried out by means of tetrahedron methods[1–3] or special-point techniques.[4–6] They use the desired quantities on a dense mesh of **k** points. The computational effort is directly related to the number of **k** points. Calculations of optical properties in crystalline semiconductors with a primitive two-atom unit cell by means of the tetrahedron method show that the number of grid points in **k** space can be reduced by a factor of 10 as compared to special-point techniques.[7,8] Nevertheless, even within the tetrahedron method a relatively high number of **k** points is desirable to obtain converged results.

In its basic version, the linear analytic tetrahedron method (LATM), the BZ is divided into tetrahedra and the band energies at the tetrahedron corners are linearly interpolated.[9,10] Consequently, the method is influenced by the band-crossing problem[9,11,12] that impedes the correct band allocation and rapid convergence. This problem is increased for systems with several hundred atoms within the unit cell. Such systems may be single crystals of complicated compounds. Typical examples are high-temperature superconductors like $YBa_2Cu_3O_{7-x}$. On the other hand, it is possible to introduce an artificial translational symmetry by choosing a large unit cell and repeating it periodically in space. The resulting supercell method is a powerful tool to treat a variety of systems without translational symmetry even within parameter-free methods of electronic structure and total-energy calculations. Supercells containing up to 216 atoms have been used in the case of defects.[13] Surfaces are modeled within the slab supercell method where a slab is repeated periodically in the direction perpendicular to the surface. The slabs are separated by vacuum. While the first *ab initio* surface calculations have been done with about 16 atoms in the unit cell,[14] today supercells of more than 100 atoms have become tractable.[15] Novel artificial materials like superlattices may be treated in much the same way. Alloys with chemical and structural disorder are described within the cluster-expansion method by studying supercells of 64 atoms fully quantum mechanically.[16] Clusters, nanocrystals, and quantum dots may also be studied using the supercell method. At present, the size of the supercells is limited to about 512 atoms.[17] This limitation is due to the huge numerical effort which also necessitates a reduction of the number of **k** points within the BZ. The systems with the largest cells can be treated restricting the calculation to only one **k** point.

In calculating spectral properties of supercell systems a number of issues become important. First of all, the two contradicting objectives of a high number of **k** points for the tetrahedron method and a smallest-possible number for the electronic-structure calculations have to be reconciled. Furthermore, according to the size of the supercell and the smallness of the BZ, a large number of bands lies in a very small energy interval. Therefore, band allocation at different **k** points is rendered utterly impossible. Additionally, spurious optical transitions occur.

In this paper we develop an extrapolative version of the tetrahedron method which can do with a single **k** point in the irreducible part of the BZ (IBZ). The problems and the efficiency of the method are demonstrated studying simple-cubic supercells of 216 and 512 atoms. As an example of a spectral property we calculate the optical absorption of a bulk semiconductor as well as of a nanocrystal embedded in this semiconductor. Moreover, we present results for the density of states and discuss the joint density of states (JDOS).

The paper is organized as follows. Section II begins with the description of the *ab initio* method used for the electronic-structure calculations and the pecularities of the use of large supercells. Then the method to describe the spectral properties of systems with huge unit cells is presented. It is based on the supercell approach, the linear analytic tetrahedron method, and a quadratic expansion of the bands. Spectral properties like optical absorption and density of states of a crystal with two atoms in the primitive

cell are considered in Sec. III to test the method. In Sec. IV it is applied to calculate the spectral properties of a Ge cluster embedded in a SiC matrix. Finally, a summary is given in Sec. V.

II. COMPUTATIONAL METHODS

A. Electronic structure calculation

The electronic band structures entering the calculations of the optical properties within the independent-particle approximation[7,8] follow from a parameter-free treatment of the supercell system within the density-functional theory (DFT) and the local density approximation (LDA). We apply the Vienna *ab initio* simulation package[18] (VASP) which employs ultrasoft (US) non-norm-conserving pseudopotentials (PP's) of the Vanderbilt type. They allow the treatment of several hundred atoms in one unit cell, even in the case of first-row elements.[19] However, for the calculation of optical properties these PP's require an augmentation of the pseudo-wave-functions in the region of the atomic cores. The formal relationship of the US-PP method[20] and the frozen-core projector-augmented wave method[21,22] (PAW) suggests the calculation of all-electron valence wave functions in the framework of the latter from the very beginning. The success of this approach for optical properties has been demonstrated recently.[23] Here we apply this method to calculate the single-particle Kohn-Sham eigenvalues $E_\nu(\mathbf{k})$ of Bloch states $|\nu\mathbf{k}\rangle$ and interband ($\nu \neq \nu'$) as well as intraband ($\nu = \nu'$) matrix elements $\langle \nu\mathbf{k}|\mathbf{p}|\nu'\mathbf{k}\rangle$ of the momentum operator $\mathbf{p}$. These states are characterized by the band index ν and a Bloch wave vector $\mathbf{k} \in \mathrm{BZ}$. Since the quanties $\{|\nu\mathbf{k}\rangle\}$ represent all-electron wave functions the optical transition operator is no longer nonlocal and can be replaced by the momentum operator, at least within the Coulomb gauge of the electromagnetic field.[7,23]

The quality of the calculations depends sensitively on the accuracy of the optical transition matrix elements and the intraband and interband momentum matrix elements used within the extrapolation procedure. In order to demonstrate the precision of the calculations within the PAW method[20,23] we study the numerical fulfillment of the relation between the intraband momentum matrix elements and the gradient of the corresponding Bloch band in $\mathbf{k}$ space, $\langle \nu\mathbf{k}|p_\alpha|\nu\mathbf{k}\rangle = (m/\hbar)(\partial/\partial k_\alpha)E_\nu(\mathbf{k})$. A comparison of derivatives obtained from these gradients to derivatives from energy differences at two $\mathbf{k}$ points in close vicinity is shown in Fig. 1. The test has been performed for the center of gravity of the tetrahedron, $\mathbf{k}_0 = (0.25,\ 0.125,\ 0.375)$, lying between $\mathbf{k}_1 = (0.250\,73,\ 0.125\,14,\ 0.375\,36)$ and $\mathbf{k}_2 = (0.249\,27,\ 0.124\,86,\ 0.374\,64)$, in units of the reciprocal basis vectors of the 8-atom simple-cubic cell which has been used. Obviously the quality of the intraband matrix-element calculation is excellent.

Throughout the paper we consider cubic SiC as an example of a zinc-blende semiconductor crystal. It is a group-IV material but occurs as a compound with partial ionic bonds. Despite the inclusion of the first-row element carbon, the plane-wave expansion cutoff can be chosen as low as 14.7 Ry.[19] This cutoff can be kept when embedded nanocrystals are treated. The nanocrystal we consider as an example consists of germanium. The core radius of Ge atoms is larger than that of Si or C atoms. The optical absorption and the DOS as well as the JDOS used as reference have been calculated for a SiC crystal with a two-atom cell and 100 conduction bands. In the IBZ a grid of 2456 $\mathbf{k}$ points and 12 685 tetrahedra have been used within the standard interpolative LATM.[10] The resulting spectra are referred to as ''reference'' in the text.

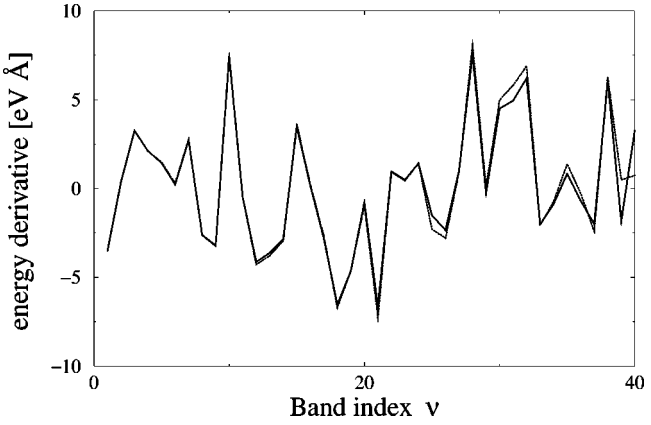

FIG. 1. Band energy derivative plotted versus the band index. Solid line: derivative derived from the momentum matrix elements; dotted line: derivative calculated geometrically from band energies. An 8-atom simple-cubic supercell is used in order to make band allocation possible. The material is SiC.

B. Supercell approach

We consider only simple-cubic supercells, both for simplicity and because in this case the number of nearest-neighbor supercells is the smallest one. When no symmetry is broken the IBZ, being one 48th part of the whole BZ, is itself a tetrahedron. A simple-cubic supercell is constructed by basis vectors $\mathbf{a}_1 = Na_0(1,0,0)$, $\mathbf{a}_2 = Na_0(0,1,0)$, and $\mathbf{a}_3 = Na_0(0,0,1)$. Here N gives the length of the supercell in multiples of the cubic lattice constant a_0 of the underlying fcc crystal. Correspondingly, the reciprocal lattice vectors are shortened by a factor of N. Applying $N = 1,2,3$, and 4 in each of the three Cartesian directions, one obtains supercells of 8, 64, 216, and 512 atoms, respectively.

The representation of a bulk material by a supercell system of artificial translation symmetry has consequences for the Bloch wave vector and the number of bands per energy interval. Instead of the reciprocal-lattice vectors $\mathbf{b}_1 = (2\pi/a_0)(1,1,-1)$, $\mathbf{b}_2 = (2\pi/a_0)(1,-1,1)$, and $\mathbf{b}_3 = (2\pi/a_0)(-1,1,1)$ the shorter ones $\mathbf{b}_1 = (2\pi/Na_0)(1,0,0)$, $\mathbf{b}_2 = (2\pi/Na_0)(0,1,0)$, and $\mathbf{b}_3 = (2\pi/Na_0)(0,0,1)$ have to be considered. Correspondingly the bands in the larger BZ are folded onto the smaller one. For instance, the original X points are folded onto the Γ point. Consequently the band structure of the indirect semiconductor SiC with the conduction-band minima at X becomes apparently direct. However, the optical matrix elements of such direct (more precisely: quasidirect) transitions at Γ vanish.

In general, as a consequence of the fact that states belonging to different **k** points in the BZ of the initial structure are folded onto the same **k** point, spurious optical transitions occur. These transitions are, however, strictly forbidden in the BZ of the ideal crystal. The number $n_{spurious}$ of spurious transitions in relation to the real ones n_{real} is easily seen to be $n_{spurious}/n_{real}=n_{cb}n_{vb}16N^3$, where n_{cb} and $n_{vb}=4$ are the numbers of conduction bands and valence bands related to the initial primitive cell of the fcc structure. Although the respective transition probabilities vanish exactly, the question arises whether the numerically nonzero transition probabilities due to inaccuracies create a computational problem. We found that the values of the transition matrix elements of a typical spurious transition is smaller by a factor of 10^{-6} than those representing real transitions. Thus, for the supercells considered in the present work one can ignore the influence of spurious transitions. However, it should be kept in mind for the future application of the method to even larger supercells.

Another problem closely related to the band-structure folding is the practical impossibility of band allocation at different **k** points. While from an analytic point of view bands are fairly well defined entities and continuous, the computational reality provides just stacks of energetically ordered values at different **k** points. The tiny separations of the energy values due to the huge number of bands within the supercell description and the occurrence of band crossings and anticrossings make apparent that the ideas of band allocation at different **k** points and, hence, also any interpolative methods have to be abandoned.

C. Tetrahedron method

Within the tetrahedron method[2,3] one has to treat sums of integrals over all tetrahedra γ of the form

$$F(\omega)=\sum_{\gamma}\int_{\gamma}d^3\mathbf{k}f(\mathbf{k},\omega), \tag{1}$$

where **k** is restricted to the tetrahedron γ. Examples for the integrands are the density of states with $f(\mathbf{k},\omega)=(4\pi^3)^{-1}\Sigma_\nu\delta(E_\nu(\mathbf{k})-\hbar\omega)$, the ν-sum running over all bands, the joint density of states with $f(\mathbf{k},\omega)=(4\pi^3)^{-1}\Sigma_{cv}\delta(E_c(\mathbf{k})-E_v(\mathbf{k})-\hbar\omega)$, and the imaginary part of the dielectric function. Within the independent-particle approximation the latter one follows from the Ehrenreich-Cohen formula[7,8]

$$f(\mathbf{k},\omega)=\frac{e^2\hbar^2}{2\pi}\sum_{c,v}\sum_{\mathbf{k}}\frac{|\langle c\mathbf{k}|p_\alpha|v\mathbf{k}\rangle|^2}{(E_c(\mathbf{k})-E_v(\mathbf{k}))^2}\times\delta(E_c(\mathbf{k})-E_v(\mathbf{k})-\hbar\omega). \tag{2}$$

For both the JDOS and the dielectric function the double sum runs over all pairs of occupied valence bands and empty conduction bands.

Within the linear analytic version of the tetrahedron method,[10] the three-dimensional integral in Eq. (1) is replaced by a surface integral which is analytically performed. The method requires the knowledge of the energy values at the tetrahedron vertices as well as the optical matrix elements appearing in expression (2) as input. The latter ones are taken to be constant over a single tetrahedron[10] or can be linearly approximated.[24] The LATM needs dispersive bands, or, in the cases of the JDOS and the dielectric function, band differences varying with the **k** vector. It will, therefore, not be capable of dealing with nondispersive bands, i.e., localized states. In such cases the corresponding contribution to the considered spectral quantity has to be related to a lifetime-broadened Dirac's δ function.

D. Extrapolation of energy bands

The interpolation of the band or band pair energies between the tetrahedron vertices requires the band allocation at different **k** points. This is practically impossible for large supercells. In conjunction with the limitation to the generation of the electronic structure at one **k** point, an extrapolative method[1,12,25,26] is needed. To obtain the energy values of the bands for one tetrahedron we start from some $\mathbf{k}_0$ and extrapolate, essentially by means of the **k·p** perturbation theory. Basically the formula we use is

$$E_\nu(\mathbf{k})=E_\nu(\mathbf{k}_0)+\frac{\hbar}{m}\langle\nu\mathbf{k}_0|\mathbf{p}|\nu\mathbf{k}_0\rangle(\mathbf{k}-\mathbf{k}_0)+\sum_{\alpha,\beta}(k_\alpha-k_{0\alpha})(k_\beta-k_{0\beta})\frac{\partial^2}{\partial k_\alpha\partial k_\beta}E_\nu(\mathbf{k})\Big|_{\mathbf{k}_0}. \tag{3}$$

The second derivatives are explicitly related by

$$\frac{\partial^2}{\partial k_\alpha\partial k_\beta}E_\nu(\mathbf{k})=\frac{\hbar^2}{m}\left\{-\sum_{\nu'}{}'\ f^{\alpha\beta}_{\nu\nu'}(\mathbf{k})+\delta_{\alpha\beta}\right\} \tag{4}$$

to the oscillator strengths

$$f^{\alpha\beta}_{\nu\nu'}(\mathbf{k})=\frac{1}{m}\frac{\langle\mathbf{k}\nu|p_\alpha|\mathbf{k}\nu'\rangle\langle\mathbf{k}\nu'|p_\beta|\mathbf{k}\nu\rangle+\langle\mathbf{k}\nu|p_\beta|\mathbf{k}\nu'\rangle\langle\mathbf{k}\nu'|p_\alpha|\mathbf{k}\nu\rangle}{E_\nu(\mathbf{k})-E_{\nu'}(\mathbf{k})}. \tag{5}$$

The gradients of the energy bands are represented by the intraband matrix elements of the momentum operator at the chosen $\mathbf{k}_0$. From this representation it is clear that we have to use a $\mathbf{k}_0$ point that does not give rise to degenerate states. That means, $\mathbf{k}_0$ cannot be a high-symmetry point, and also cannot lie on a symmetry plane or line. For this reason, in the

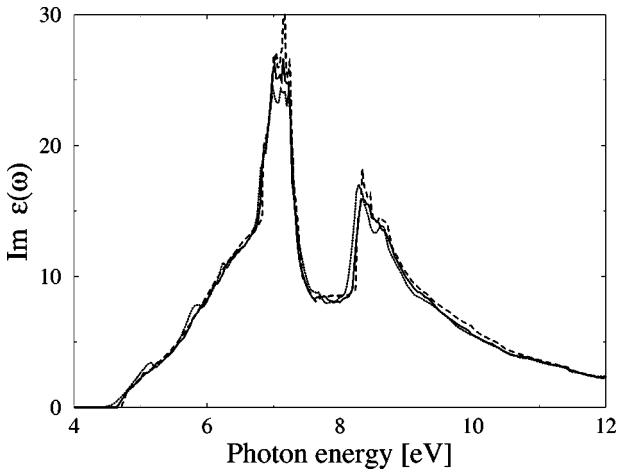

FIG. 2. Imaginary part of dielectric function of SiC for linearly (dotted) and quadratically (solid line) extrapolated energies for a 512-atom SiC supercell. 2048 bands are used and the IBZ is divided into 64 tetrahedra. The converged reference result is given as a dashed line.

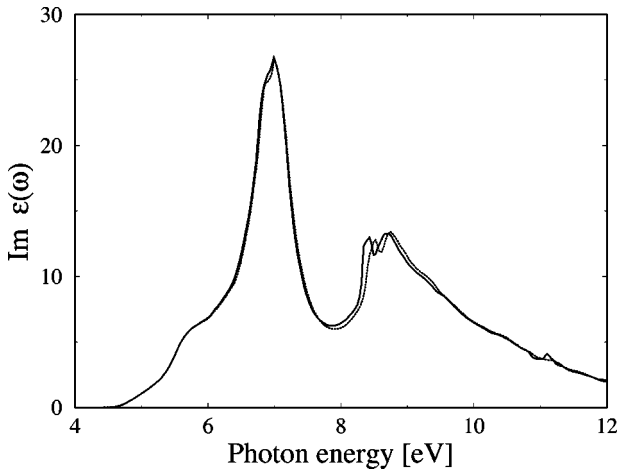

FIG. 3. Dependence of the dielectric function on the number of bands. Only the effect on the energy extrapolation is shown. The perturbative determination of the vertex energies is carried out with 1296 (solid line) and 864 bands (dashed line), whereas the calculation of the dielectric function was restricted to 864 bands in both cases. A 216-atom SiC supercell is used.

simple-cubic case $\mathbf{k}_0$ should not be identified with the Baldereschi point.[4] We use the center of gravity of the IBZ, which is itself one tetrahedron, as the $\mathbf{k}_0$ point.

III. NUMERICAL DETAILS: IDEAL CRYSTAL

A. Linear versus quadratic extrapolation

Keeping only the gradient term in Eq. (3) one obtains a linear approximation of the band structure. However, this approach does not work at critical points $\mathbf{k}$. Because of the symmetry the bands have to be flat there, whereas the linear extrapolation from $\mathbf{k}_0$ remarkably overestimates the band energy correction at $\mathbf{k}$. Thus, as a major drawback of the linear extrapolation, the bands are especially poorly represented at tetrahedron vertices coinciding with critical points.

Despite these limitations the optical absorption of cubic SiC is well represented in Fig. 2 in comparison to the result of the quadratic extrapolation and the reference spectrum. Nevertheless, all band energies at the corresponding tetrahedron vertices have been calculated according to expression (3) and starting from the single point $\mathbf{k}_0$ in the center of the IBZ. The restriction to the linear extrapolation gives rise to additional unphysical structures on the low-energy side of the main absorption peak and an onset of the absorption below the smallest allowed direct transition. On the other hand, the quadratic extrapolation (with resampling—see below) gives a reliable spectrum. Only the intensity of the main absorption peaks would slightly be underestimated.

B. Sum over bands

The quadratic term in Eq. (3) contains the usual second-order perturbation sum over all bands as indicated by the relation to the oscillator strengths in expression (4). The truncation of this sum is computationally inevitable. Its effect, however, has to be tested carefully. Furthermore, for the large-supercell systems the energies lie so dense that the sum effectively becomes an integral. In fact, the energy separations are frequently smaller than the precision of the energies. Since an intraband contribution does not occur, the sum can be replaced by an integral in the sense of the Riemann definition. The principal value is computed in practice by adding a small imaginary part $i\delta$ to the energy nominator and considering the real part. It turns out that the method is fairly insensitive with respect to the choice of the parameter δ. Between the two extremes where either the second-order energy terms scatter strongly due to a too small δ, or the result starts losing structures due to a too large δ, there is a rather wide region for the broadening parameter over which the result does not change appreciably. Our experience indicates that it is best to choose the parameter as small as possible but without a singular tail arising towards $\hbar\omega=0$. Reliable values are $\delta=0.001$–0.1 eV for 216-atom cells and $\delta=0.000\,01$–0.01 eV for 512-atom cells.

The accuracy of the second-order expansion of the energy bands (3) also depends on the number of conduction bands. The number of bands taken into account influences the results in two ways. First, one has to include all optical transitions which are relevant at a certain photon energy in the spectrum. A test reveals that very few conduction bands are necessary to represent the main part of the absorption spectrum except for the high-energy tail. As few as four conduction bands are able to account correctly for the dielectric function up to 12 eV for a system with two atoms in the unit cell. In the case of the 512-atom cell this corresponds to the use of 1024 conduction bands.

Second, the number of bands influences the convergence of the perturbation series in expression (4). The ''repulsion of the bands'' due to their interaction requires the inclusion of a reasonable number of bands above the considered one. Consequently, for the higher bands the second-order energy correction will be less accurate than for the lower ones, and the resulting error will be systematic. Figure 3 shows that this is really the case. The same calculation has been done

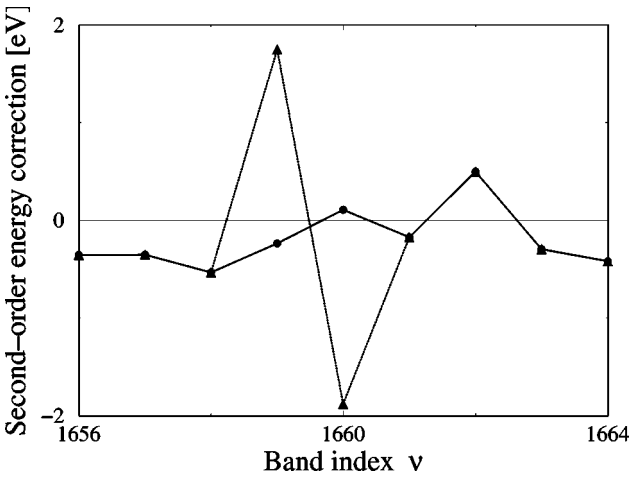

FIG. 4. The second-order energy term before (dotted line, triangles) and after (solid line, circles) the kissing correction plotted versus the band index. The bands 1659 and 1660 participate in a kissing, indicated by the extreme values of the second-order energy correction. A 512-atom cell is considered.

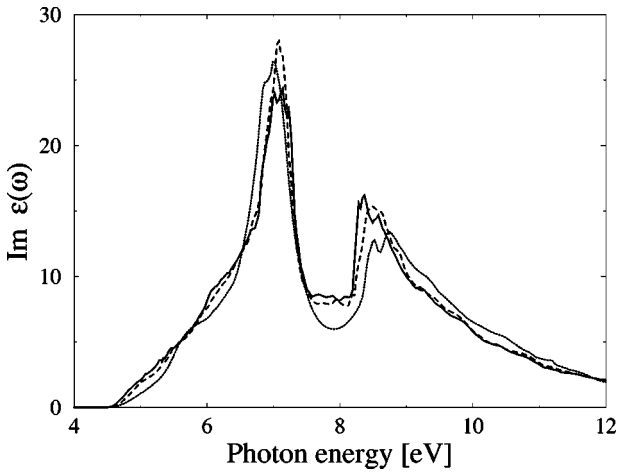

FIG. 5. Imaginary part of the dielectric function for 216-atom cell and three resampling densities. Different numbers of tetrahedra are generated within the irreducible part of the BZ. 1: dotted line; 8: dashed line; 512: solid line.

for different numbers of conduction bands taken into the perturbation sum in Eq. (4). However, for the calculation of the absorption in both cases the same number of bands were used. For the higher number of included bands the high-energy absorption peak slightly changes its location towards the reference value.

There is another point of importance. Perturbation theory requires the energy corrections to be smaller than the difference of the involved unperturbed energy levels. For the large extrapolation distances $(\mathbf{k}-\mathbf{k}_0)$ that we have to deal with, this condition is poorly fulfilled, at best. In this sense we have to state clearly that by means of equation (3) we do not, strictly speaking, calculate a well-defined perturbative expansion but rather a geometrical extrapolation from the first and second derivatives of the energy bands at $\mathbf{k}_0$. Thereby we do heavily rely on the smooth behavior of the bands. In other words, viewed as a perturbative calculation the convergence properties could not be assured. However, our results clearly indicate the viability of extrapolation in the face of this problem.

Nevertheless, we have to discuss the question of how well even exact second-order extrapolation can describe the bands, i.e., how dangerous is it for a particular band to drop the basic requirement of perturbation theory? This problem is exemplified by what Pickard and Payne call ''band kissing,''[12] also known as anticrossing. The effect occurs when two bands which would truly intersect each other are ''repelled'' by their interaction. This repulsion causes extreme values of the second-order energy derivatives for the respective two bands which are limited to the immediate vicinity of the anticrossing. If $\mathbf{k}_0$ happens to be very close to such a point, the second-order energy corrections to the two bands will be much too large, similar in value, and have opposite signs.[12] This can be seen in Fig. 4 where the second-order energy correction is plotted as a function of the band index. In the simplest possible case of just two bands, the problem can be solved by using $\mathbf{k}\cdot\mathbf{p}$ theory for almost degenerate bands[27] and crossing the bands ''by hand'' by an assignment of the new energy values such that smooth, crossed bands are obtained. We found that it is possible to look for extreme values of the second-order energy terms which are close in terms of the band indices and similar in size but have different signs. We only check those for the direction of highest curvature and apply the method of Pickard and Payne[12] to them. The result of such a treatment is also demonstrated in Fig. 4. However, at least in the cases we considered, the band-kissing effect on the overall result is negligible. Within the precision of our calculations the correction can safely be neglected.

C. Convergence: Resampling and cell size

In principle, the availability of the quadratic representation of the band structure around some $\mathbf{k}_0$ allows the application of the analytic quadratic tetrahedron method.[28] However, in view of the errors incurred from our extrapolation, the effort necessary to implement the quadratic method, and the existence of a code and expertise about the linear method we retain the linear method.

In order to diminish the obvious problem of committing the systematic error of linearly interpolating a quadratic function between two fairly distant points in $\mathbf{k}$ space we introduce a resampling procedure. We subdivide the tetrahedron representing the irreducible part of the BZ into smaller ones and calculate the energies at their corners according to expression (3). We use meshes of 1, 8, 64, 512, and 4096 tetrahedra. Resulting spectra are shown in Fig. 5 for SiC in a 216-atom cell. There is clearly an improvement of the absorption spectrum with increasing number of tetrahedra. The use of 512 tetrahedra gives already a converged result. Further subdivision of the tetrahedra does not lead to further improvement. Apart from the fine structure of the two main absorption peaks, the 512-tetrahedra result already approaches the reference spectrum (not shown in Fig. 5 to avoid confusion).

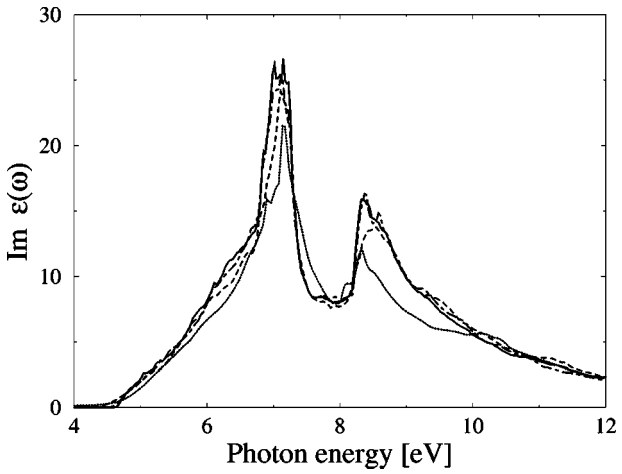

FIG. 6. Imaginary part of the dielectric function of SiC calculated for different supercell sizes. 8 atoms: dotted line; 64 atoms: dashed line; 216 atoms: dot-dashed line; 512 atoms: solid line.

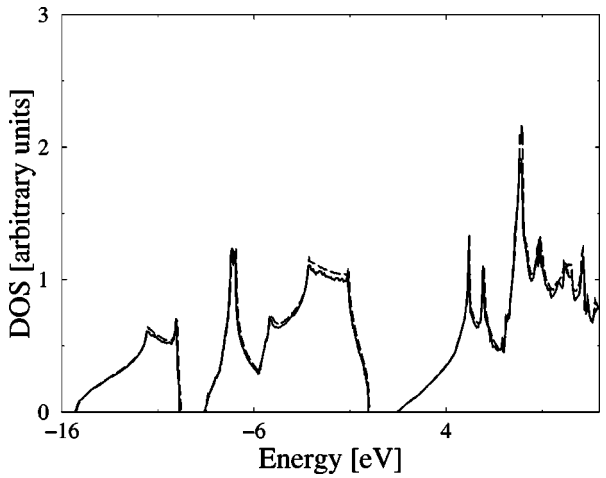

FIG. 7. Density of states as calculated by means of the 512-atom supercell (solid line), compared to the reference (long-dashed line).

The question arises which supercell sizes our method is applicable to. The larger the real-space cell, the smaller is the BZ, and, consequently, the shorter are the extrapolation distances in **k** space. The SiC results are shown in Fig. 6 for supercells containing 8, 64, 216, and 512 atoms, respectively. In all cases a 64-tetrahedra resampling has been employed. It is apparent that for the 8-atom cell the extrapolation distances are as large as to only allow a representation of the main features of the optical absorption spectrum in a crude manner. The method works much better in the 64-atom cell, although in this case it is still rather far from convergence. For the two largest cells under consideration the method gives a more or less well converged absorption spectrum. In the largest cell with 512 atoms the spectrum is in excellent agreement with the reference result, apart from a small underestimate of the heights of the main absorption peaks.

As a further demonstration of the quality of the extrapolation method starting from only one $\mathbf{k}_0$ point we calculate the DOS of SiC in the 512-atom cell with a 64-tetrahedra resampling. This is a very good indicator of the quality of the energy extrapolation because it involves only the energies, not, however, the transition matrix elements. It is clearly demonstrated in Fig. 7 that our method of using only one $\mathbf{k}_0$ point in the IBZ is capable of yielding excellent results for spectral properties.

D. Spurious transitions

We turn back to the discussion of the spurious optical transition. While the meaning of the DOS is and remains clear, the JDOS incurs arbitrariness in the case of large supercells, i.e., a nonprimitive unit cell. Depending upon how often the BZ has been folded, the JDOS fully counts the spurious transitions, i.e., seemingly direct transitions which, however, represent transitions between states at different points of the BZ before folding. They do not influence the computation of the dielectric function because the contribution of each optical transition in Eq. (2) is weighted by the oscillator strength $f_{cv}^{\alpha\alpha}(\mathbf{k})$ in expression (5). On the other hand, the spurious transitions count fully for the JDOS. Therefore, as long as one does not restrict the treatment to primitive unit cells, one is faced with ambiguity in the JDOS treatment. The problem persists as long as one considers supercell arrangements without any disturbance of the ideal crystal structure. While the physical properties approach those of the pure bulk material, the JDOS obviously does not. It is clear from that argument that the JDOS is not to be counted among the observable quantities like the DOS and the dielectric function.

This raises the question if there is a way to recover the original ''true'' JDOS of the ideal crystal from the supercell description. To achieve this one has to disregard those spurious transitions. As the parameter to decide whether or not a contribution of an electron-hole pair at a certain **k** point is counted for the JDOS we insert the requirement that the oscillator strength of a given transition is larger than some cutoff strength f_0. Results for SiC are shown in Fig. 8 where the JDOS calculated for a two-atom cell is compared to that from the 512-atom cell. Evidently the procedure has at least some merit. There is a broad region of the cutoff parameter for which the spectra do not change remarkably.

Moreover, up to about 8 eV the spectra shown in Fig. 8 are rather insensitive to the particular choice of the cutoff and, hence, extremely close to the reference one. For the crystal with two atoms in the primitive cell, on the one hand this means that the spurious transitions are well taken off the summation. On the other hand, the influence of ''real'' transitions, i.e., transitions also occurring in the primitive-cell description, but having vanishing transition probabilities, is very weak. For energies above 8 eV the ambiguity cannot be compensated for by the cutoff anymore. This may be related to the free-electron-like behavior of the higher conduction bands giving rise to small oscillator strengths which can hardly be classified by a simple cutoff parameter.

E. Matrix element extrapolation

For the calculation of the dielectric function (2) not only the energy bands but also the transition matrix elements are

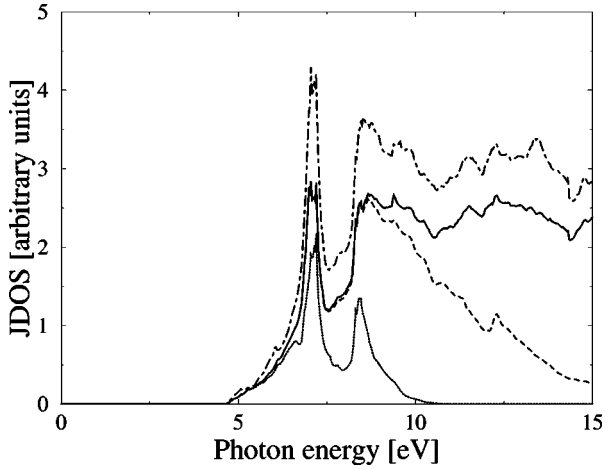

FIG. 8. Joint density of states for different cutoff parameters f_0 of the oscillator strengths. The calculation has been carried out for SiC in a nonprimitive 512-atom supercell. The solid line gives the reference result. $f_0=10^{-8}$: dot-dashed line; $f_0=10^{-4}$: solid line; $f_0=0.1$: dashed line; $f_0=0.5$: dotted line.

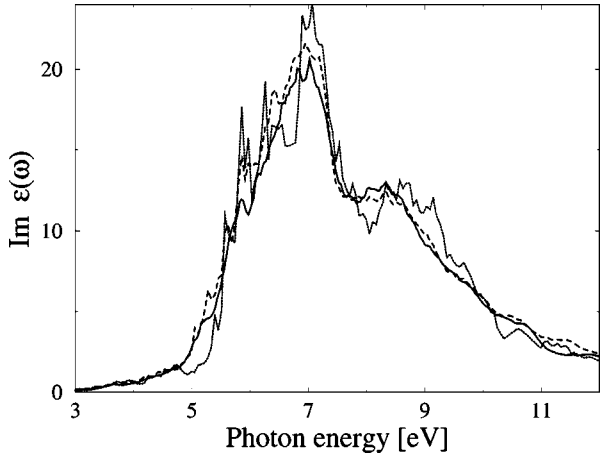

FIG. 9. Imaginary part of the dielectric function of a 41-atom Ge cluster embedded in SiC (solid line). Results of a Lorentzian broadening of the δ function with ten Monkhorst-Pack grid points in the IBZ (dashed line) as well as of the same method using only the Baldereschi point (dotted line) are also given. A broadening parameter $\Gamma=0.2$ eV and a 216-atom cell are used.

needed. These are the same matrix elements as those needed to calculate the $\mathbf{k}\cdot\mathbf{p}$ expansion (3). According to the perturbative representation of the wave functions at $\mathbf{k}$, the optical matrix elements can be extrapolated using only the momentum matrix elements at $\mathbf{k}_0$ which have been calculated anyway. Explicitly the matrix elements of the momentum operator at the tetrahedron corners are computed using the first-order $\mathbf{k}\cdot\mathbf{p}$-perturbed states. In this way the first-order matrix elements at the corners are expressed as sums of momentum matrix elements at $\mathbf{k}_0$.

As in the case mentioned above, cf. Eq. (4), the sum over bands has to be treated as a principal value integral. The variation of the matrix elements can now be included into the method using the formulas of Ren and Harrison[24] or by using different averaged values for the different tetrahedra after the resampling procedure. Otherwise, the advantage of the better description at the corners is lost because the linear inclusion of matrix-element variations amounts to averaging in the case when $\mathbf{k}_0$ lies at the center of the region under consideration. The extrapolation of the matrix elements does not change the optical absorption appreciably. Since it is very time consuming (due to the triple sum over all bands), and in view of the quality of the results without it, we conclude that for practical purposes it is reasonable to dispense with the extrapolation of the matrix elements. Any further effort to refine the method should be directed at the band structure, not at the matrix elements.

IV. APPLICATION: EMBEDDED NANOCRYSTAL

We apply the method to the calculation of the optical properties of embedded nanocrystals. To keep translational symmetry, a three-dimensional periodic arrangement of nanocrystals embedded in a matrix material is considered. In this case the supercell is the primitive unit cell of the system. Therefore the concepts of band folding and spurious transitions are only of approximate validity. An indication of that is given introducing a cutoff in the calculation of the JDOS as described above. In the case of embedded clusters there is no clear-cut separation between real and spurious transitions as in the bulk case. Instead, all transitions are real in this sense as soon as the supercell contains a perturbation of the translational symmetry of the lattice of the matrix. Consequently, the interval over which the cutoff can be varied without changing the JDOS appreciably is much smaller compared to the ideal crystal case.

As examples we consider a spherical Ge cluster of 41 atoms embedded in cubic SiC in a 216-atom or 512-atom simple-cubic supercell. The Ge atoms are kept at the former host material sites. The parameter δ for the principal value integral of the energy perturbation sum has to be chosen somewhat bigger (about $\delta=0.1$ eV) than in the bulk SiC case, presumably because the truncated basis of the perturbation expansion does not represent the localized states at the cluster as well as the delocalized bulk states.

The resulting imaginary part of the dielectric function is plotted in Fig. 9. It shows the well-known main absorption peaks of SiC around 7 and 8.6 eV (within DFT-LDA) as well as a strong change compared to the pure SiC result. The germanium dot induces a shoulder at about 6.0 eV and an extended tail below 5 eV. In Fig. 9 we also show how the spectrum computed within the extrapolation method using only one $\mathbf{k}_0$ point compares to a method[8] where Lorentzian-broadened Dirac's δ functions calculated for a dense Monkhorst-Pack mesh of ten $\mathbf{k}$ points are summed up. We suppose the ten $\mathbf{k}$-point result to be converged with respect to the number of $\mathbf{k}$ points. While this can be taken as a reference for the optical properties of the artificial dot-host lattice system, it is also possible to compare to Baldereschi-point sampling, i.e., sampling at only one $\mathbf{k}$ point. This spectrum is also included in Fig. 9. Obviously our method does not fare too badly, even though the 216-atom cell is not yet quite of the preferred size. However, due to the much larger requirements of computational resources it was not possible

to obtain results using a similar high-density Monkhorst-Pack sampling for the 512-atom case.

Despite the reasonable results for Ge nanocrystals embedded in a SiC matrix, a word of caution is in order. The success of the application of the extrapolative tetrahedron method relies on the type-II heterostructure behavior of the Ge-SiC system.[17] Embedding Ge in a cubic SiC matrix gives rise only to a confinement of the holes in the nanocrystals. In spite of the small interaction between neighboring supercells the corresponding bands are fairly flat, rather like quantum levels. On the other hand, there are no confined empty states. In other words, all conduction bands exhibit dispersion. Consequently, the resulting interband energies also exhibit dispersion. In the case of type-I heterostructure systems one expects level-like lowest conduction bands. For optical transitions between such flat bands we recommend a special treatment simply by taking the respective transitions out of the tetrahedron method and applying a certain broadening of the energy-conserving δ function.

V. SUMMARY

We have developed an extrapolative method for the calculation of optical response functions, the density of states, and the joint density of states for large-supercell systems. The method is based upon the tetrahedron method. It only needs the electronic-structure calculations to be done at one $\mathbf{k}$ point $\mathbf{k}_0$ in the irreducible part of the Brillouin zone of the supercell arrangement. The transition energies at the vertices of the tetrahedron are computed using a quadratic extrapolation based on $\mathbf{k}\cdot\mathbf{p}$ perturbation theory. Both the linear and the quadratic term are related to matrix elements of the momentum operator. Hence, the same matrix elements that have been computed for the optical part of the calculations are used for the band-structure representation. The results are substantially more accurate than those restricted to a linear extrapolation of band energies. Our method allows the treatment of systems represented by arrangements of extremely large supercells. Due to the use of only one $\mathbf{k}$ point the optical calculations remain tractable for systems for which several thousands of bands have to be taken into account.

The influences of the different effects on the spectral properties have been investigated. The tests showed that the quality of the intraband momentum-matrix elements is high. This allows us to judge the wave functions and the interband matrix elements themselves, both being calculated by means of the PAW method. The influence of the kissing corrections after Pickard and Payne[12] was found to be negligible at the present level of precision, much as the linear extrapolation of the matrix elements which we introduced. We have shown the possiblity of recovering the original joint density of states of bulk material by inserting a cutoff parameter in order to disregard spurious transitions. The lower part, up to 10 eV, of the JDOS of the ideal SiC crystal has proven rather insensitive to this parameter.

The effect of the cell size and, therefore, the extrapolation distances, has been tested, as has been the resampling procedure. In the case of nanocrystals embedded in a semiconductor matrix we have compared the results of our method with those obtained by sampling methods. The extrapolative method is rather powerful to describe the spectral properties of composite supercell systems with a minimum set of $\mathbf{k}$ points.

ACKNOWLEDGMENTS

This work was financially supported by the Deutsche Forschungsgemeinschaft (Sonderforschungsbereich 196, Project No. A8). We acknowledge interesting discussions with Birgit Adolph.

[1] G. Gilat and L. J. Raubenheimer, Phys. Rev. **144**, 390 (1966).
[2] O. Jepsen and O. K. Andersen, Solid State Commun. **9**, 1763 (1971).
[3] G. Lehmann and M. Taut, Phys. Status Solidi B **54**, 469 (1972).
[4] A. Baldereschi, Phys. Rev. B **7**, 5212 (1973).
[5] D. J. Chadi and M. L. Cohen, Phys. Rev. B **8**, 5747 (1973).
[6] H. J. Monkhorst and J. B. Pack, Phys. Rev. B **13**, 5188 (1976).
[7] B. Adolph, V. I. Gavrilenko, K. Tenelsen, F. Bechstedt, and R. Del Sole, Phys. Rev. B **53**, 9797 (1996).
[8] O. Pulci, G. Onida, A. I. Shkrebtii, R. Del Sole, and B. Adolph, Phys. Rev. B **55**, 6685 (1997).
[9] P. E. Blöchl, O. Jepsen, and O. K. Andersen, Phys. Rev. B **49**, 16 223 (1994).
[10] D. J. Moss, J. E. Sipe, and H. M. van Driel, Phys. Rev. B **36**, 1153 (1987).
[11] J. E. Müller and J. W. Wilkins, Phys. Rev. B **29**, 4331 (1984).
[12] C. J. Pickard and M. C. Payne, Phys. Rev. B **59**, 4685 (1999).
[13] A. Zywietz, J. Furthmüller, and F. Bechstedt, Phys. Rev. B **59**, 15 166 (1999).
[14] M. Schlüter, J. R. Chelikowsky, S. G. Louie, and M. L. Cohen, Phys. Rev. B **12**, 4200 (1975).
[15] W. G. Schmidt, E. L. Briggs, J. Bernholc, and F. Bechstedt, Phys. Rev. B **59**, 2234 (1999).
[16] S. Mankefors and S. P. Svensson, J. Phys.: Condens. Matter **12**, 1223 (2000).
[17] H.-Ch. Weissker, J. Furthmüller, and F. Bechstedt, Phys. Status Solidi B **224**, 769 (2001).
[18] G. Kresse and J. Furthmüller, Comput. Mater. Sci. **6**, 15 (1996).
[19] J. Furthmüller, P. Käckell, F. Bechstedt, and G. Kresse, Phys. Rev. B **61**, 4576 (2000).
[20] G. Kresse and D. Joubert, Phys. Rev. B **59**, 1758 (1999).
[21] P. E. Blöchl, Phys. Rev. B **50**, 17 953 (1994).
[22] H. Kageshima and K. Shiraishi, Phys. Rev. B **56**, 14 985 (1997).
[23] A. Adolph, J. Furthmüller, and F. Bechstedt, Phys. Rev. B **63**, 125108 (2001).
[24] S. Y. Ren and W. A. Harrison, Phys. Rev. B **23**, 762 (1981).
[25] M. Taut, Phys. Rev. B **57**, 2217 (1998).
[26] C. J. Pickard and M. C. Payne, Phys. Rev. B **62**, 4383 (2000).
[27] J. P. Loehr, Phys. Rev. B **52**, 2374 (1995).
[28] M. H. Boon, M. S. Methfessel, and F. M. Müller, J. Phys. C **19**, 5337 (1986).